ACS OMEGA

http://pubs.acs.org/journal/acsodf

Article

Enhanced Antioxidant Effects of Naringenin Nanoparticles Synthesized using the High-Energy Ball Milling Method

Anas Ahmad, Ravi Prakash, Mohd Shahnawaz Khan, Nojood Altwaijry, Muhammad Nadeem Asghar, Syed Shadab Raza,* and Rehan Khan*

Cite This: *ACS Omega* 2022, 7, 34476−34484

Read Online

ACCESS | Metrics & More | Article Recommendations | Supporting Information

ABSTRACT: Naringenin, one of the flavonoid components, is majorly found in and obtained from grapefruits and oranges. Naringenin also acts as a potent antioxidant, which possesses hypolipidemic as well as anti-inflammatory potential. Naringenin reduces the expressions of several inflammatory mediators, viz., NF-κB, cycloxygenase-2, and other cytokine mediators. In spite of having various biological effects, the clinical application of naringenin is restricted due to its very poor aqueous solubility. In the present study, the high-energy ball milling method was employed for the preparation of naringenin nanoparticles without using any chemical with an aim to enhance the anti-oxidant potential of naringenin. The milled naringenin nanoparticles were characterized for their physicochemical properties using scanning electron microscopy (SEM) and X-ray diffraction. Additionally, the effects of milling time and temperature were further assessed on the solubility of crude and milled naringenin samples. The antioxidant potential of milled naringenin was evaluated with various assays such as DHE, DCFDA, and cleaved caspase-3 using SH-SY5Y human neuroblastoma cells. The nanoparticle size of naringenin after milling was confirmed using SEM analysis. Crystalline peaks for milled and crude samples of naringenin also established that both the naringenin forms were in the crystalline form. The solubility of naringenin was enhanced depending on the milling time and temperature. Moreover, crude and milled naringenin were found to be cytocompatible up to doses of 120 μM each for the duration of 24 and 48 h. It was also observed that milled naringenin at the doses of 1, 2, and 5 μM significantly reduced the levels of reactive oxygen species (ROS) generated by H_2O_2 and exhibited superior ROS scavenging effects as compared to those of crude or un-milled forms of naringenin. Furthermore, milled naringenin at the doses of 1 and 2 μM inhibited H_2O_2-induced cell death, as shown by immunofluorescence staining of cleaved caspase-3 and Annexin-V PI flow cytometry analysis. Conclusively, it could be suggested that the size reduction of naringenin using high-energy ball milling techniques substantially enhanced the antioxidant potential as compared to naïve or crude naringenin, which may be attributed to its enhanced solubility due to reduced size.

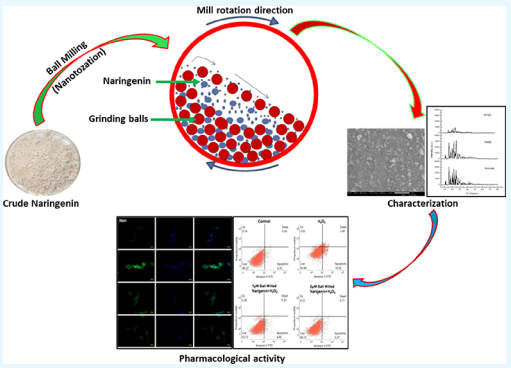

1. INTRODUCTION

Nanoparticle-based formulations and drug delivery platforms have drawn much attention because of their discrete and special characteristic features, which are quite limited in present-day conventional drugs and medicines. For example, the reactivity of nanoparticulate materials with other biological milieu has been comparatively more efficient and effective because of the higher surface-to-volume ratio, along with the higher number of atoms reacting on the surfaces and at other interfacial regional boundaries. Several studies have described the biomedical applications of nanoparticles, mainly as anti-microbial nanoformulations, in cellular and other bio-imaging techniques, drug-delivering paradigms, and anti-cancer therapies.[1−3]

Naringenin is one of the chief citrus flavonoid components, majorly ascertained among grapefruits and oranges, and possesses structural similarity to widely researched polyphenolic compound resveratrol. Naringenin is also a potent antioxidant, which possesses hypolipidemic and anti-inflammatory potential.[4,5] This flavonoid compound has shown quite strong protecting efficacies against atherosclerotic disorders, although the particular mechanism implicated in these effects has not been totally explored.[6,7] In one clinical study, this flavonoid substance could cause the reduction of circulating low-density lipoprotein (LDL) levels by 17% in patients having hypercholesterolemia.[8] Naringenin also possesses strong anti-inflammatory potential, which reduces expressions of several inflammatory mediators, viz., NF-κB, cycloxygenase-2, and other cytokine mediators.[9] Several other pharmacological

Received: July 1, 2022
Accepted: September 7, 2022
Published: September 19, 2022

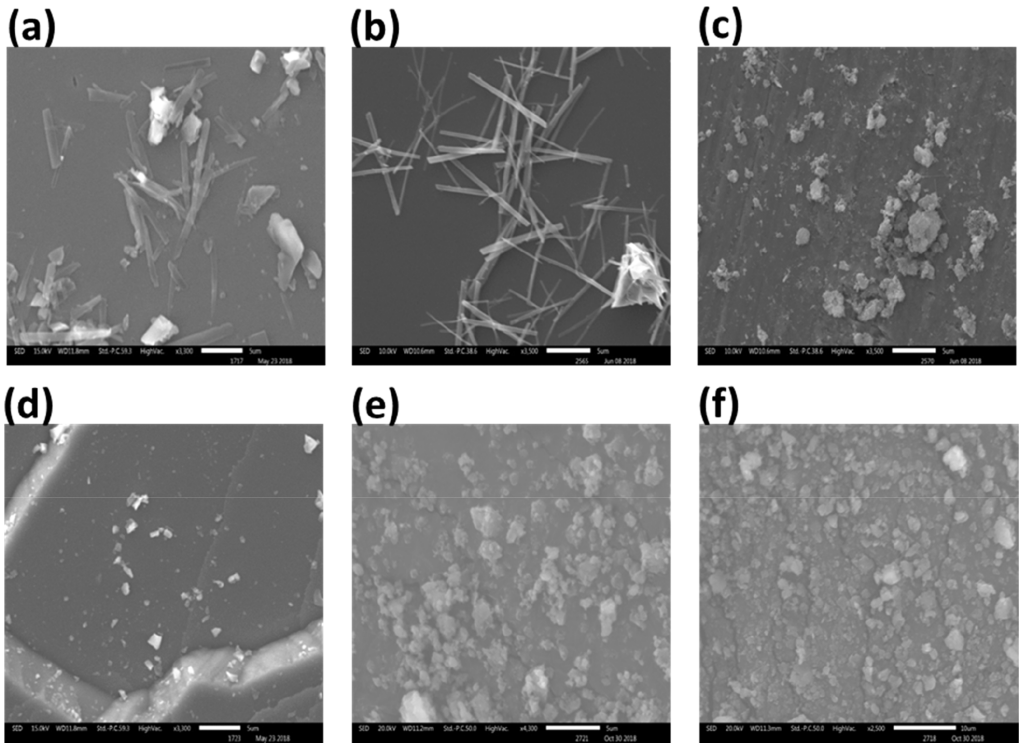

Figure 1. SEM images of naringenin at different milling times; here (a) unprocessed naringenin, (b) naringenin after 120 min of milling, (c) naringenin after 240 min of milling, (d) naringenin after 480 min, (e) naringenin after 600 min of milling, and (f) naringenin after 720 min of milling.

actions have been ascribed to naringenin, which includes anti-tumorigenic action, anti-angiogenesis capacity, and other neuroprotective actions.[10−12]

Because of the quite poor water solubility of naringenin (9.80 μg/mL at room temperature) which ultimately results in highly inefficient delivery and poor pharmacological performance, several efforts have been made for the customization and synthesis of naringenin nanoformulations in general and nanoparticles in particular for various applications.[10,13,14] The ultimate aim of the conversion of the conventionally available micro-form of naringenin into its nanosized formulation is the enhancement of its saturation solubilities and increased drug absorption through various cellular and tissue surfaces, culminating into the higher bioavailability.

Although these nano-conversion techniques have seen some success rates, most of these suffer from one or the other limitations, which include poor yields, lower purity rates, lower biocompatibility, and higher toxicity concerns. Therefore, a low-temperature, larger-scale and simpler nanoformulation process is required for synthesizing the nanocrystalline form of naringenin nanoparticles.

Recently, mechanical ball milling has been reported to be an effective and simpler process without implicating the high-temperature treatments for producing the nanocrystalline formulations of powders, and higher yields are expected with larger quantities of nanoparticles and customized characteristic features.[15−17] Here, in this methodology, initially powdered particles get entrapped among the extremely energizing jarring metallic balls and interior boundaries of vials, which then leads to recurring contortion, rewelding, and breaking down of pre-mixed powdered materials culminating into the formulation of finer, discrete nanoparticles in these matrices. During this milling technique, two necessary actions impact nanoparticles' characteristic features.[17,18] First, the cold-welding phenomena results in an enhancement in the mean nanoparticle size. Second, the fragmenting action leads to the breaking up of complex particulate materials. Steady-state equilibria are obtained when the balancing is accomplished among these actions beyond a particular duration of ball milling.[17] The chief application of present-day ball milling is the fracturing of micro-particles and reducing their particle size, which becomes quite distinct from the newer high-energy ball milling technique.

Therefore, with regard to the significance of ball milling methodology in nanoparticle formation and then alteration of their physicochemical characters, this technique was applied in naringenin nanoparticle formation. In this study, various structural [X-ray diffraction (XRD)], microscopic [scanning electron microscopy (SEM)], and other biological analyses were carried out on the formulated naringenin nanoparticles. All these analyses demonstrated quite significant results on this drug material, which may be of appreciable applications in many arenas like nanoparticle-mediated targeting of diseases and disorders. To the best of our knowledge, this is the first study where nanosized naringenin obtained after the ball milling method has been employed for the reduction of reactive oxygen species (ROS) in the cells in vitro model, viz., its safety in terms of biocompatibility has been tested in hTERT-BJ cell lines and pharmacological efficacy has been tested in the SH-SY5Y human neuroblastoma cell line.

2. MATERIALS AND METHODS

The materials and method sections have been provided with a detailed description in the Supporting Information file.

https://doi.org/10.1021/acsomega.2c04148
ACS Omega 2022, 7, 34476−34484

3. RESULTS AND DISCUSSION

In the recent past, several studies have reported the ball milling of naringenin for the conversion of naringenin into its nanoparticle forms, and these studies have been added in the Discussion Section.[19−22] The clinical and therapeutic efficacy of naringenin is restricted due to its lower bioavailability because of the poor solubility. For the enhancement of its solubility, naringenin nanosuspension was prepared by the milling technique. The nanoparticle size, surface morphology, and so forth were evaluated, and stability studies were also assessed by observing the particle size alterations in various physiological media.[19] Similarly, a high-energy ball milling technique was used to prepare nano-naringenin, which was characterized with the help of transmission electron microscopy followed by the assessment of pharmacological efficacy of nanosized naringenin in the amelioration of the biochemical, behavioral, and histological changes induced by the nicotine in rats.[20] Another report aimed to formulate the stable nanosized naringenin by the milling methods and exploring its potential applicability for rheumatoid arthritis. Physiochemical properties, physical stabilities, and dissolution functioning of nanosized naringenin were evaluated. Intracellular uptake and transportation of nanosized naringenin were subsequently assessed in Caco-2 cells. Finally, in vivo pharmacokinetics and anti-inflammatory potential of nanosized naringenin were also evaluated. The outcomes of all these experiments provided newer insight into the treatment of rheumatoid arthritis.[21] Another study describes the formulation and assessment of naringenin nano-suspensions for enhancing bioavailability. This top-down approach undertakes the application of high-energy ball milling methods for the reduction of nanoparticle size to enhance the saturation solubility of naringenin, ultimately improving its bioavailability.[22]

The present approach was basically undertaken to convert the naive or microcrystalline form of the naringenin drug into its nanocrystalline form with the aid of the ball milling technique. In the recent past, a number of different tools and techniques have been employed for either the mechanosynthesis of nanoparticles by ball milling or the conversion of microcrystalline forms of the materials to their nanocrystalline forms and variants.[23−28] In the present study, ball milling of the crude or naive form of microcrystalline powder of naringenin was carried out for various time intervals, and at each time point, a sample was taken for the size, shape, and morphological characteristic analyses of the milled samples by SEM (Figure 1). A number of reasons could be attributed to the enhanced pharmacological efficacy of bioactive compounds after their size reduction. One of the chiefs and prominent reason is the increase in the saturation solubility, and distribution rates, and as result an overall improvement in the bioavailability of the nanoparticulate form of the bioactive compound under investigation.[29−31] This also seems to be the

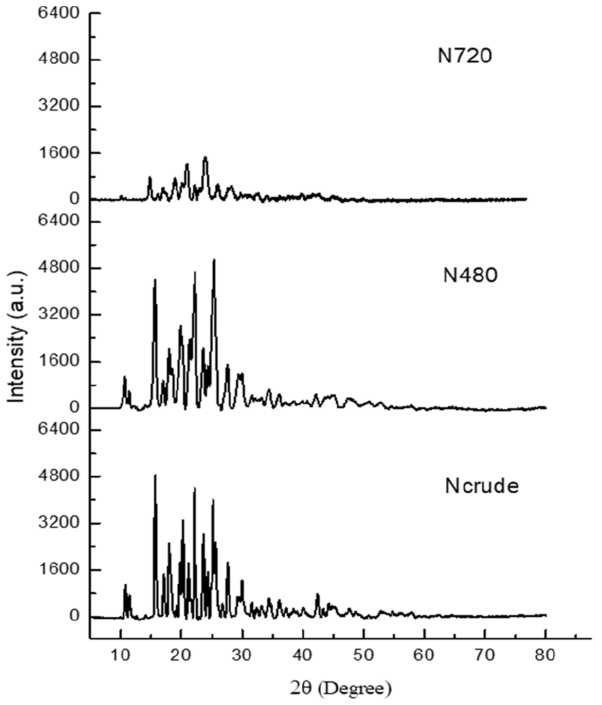

Figure 2. X-ray diffraction patterns of naringenin at milling time; Ncrude (not processed), N480 (after 480 min of milling), and at N720 (after 720 min of milling).

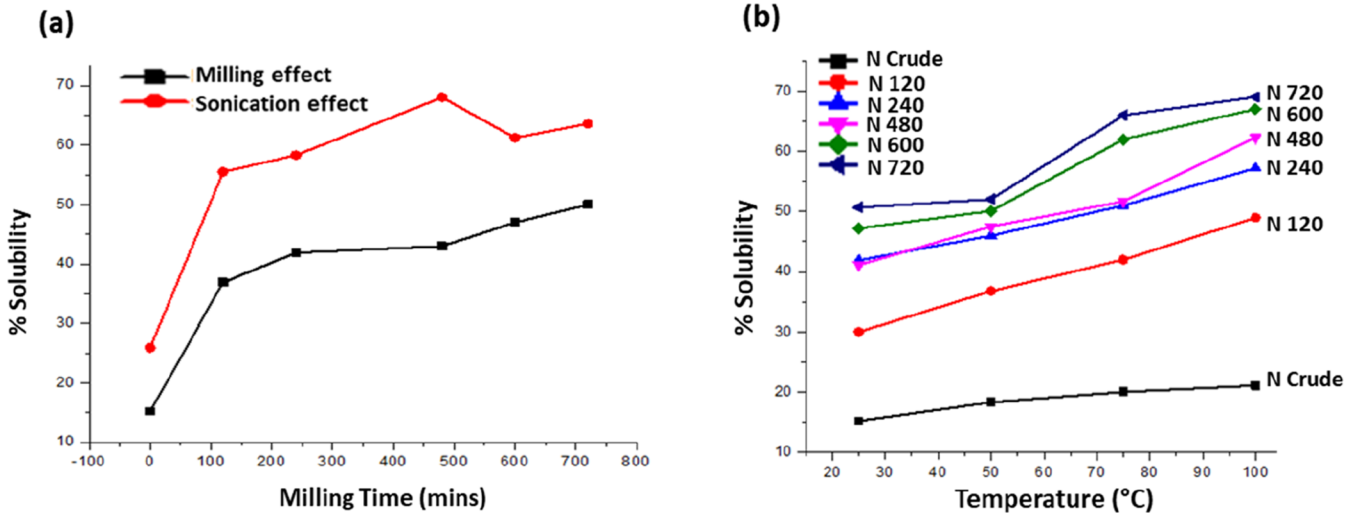

Figure 3. (a) Solubility values of crude and milled naringenin samples (black) without sonication and solubility values of crude and milled naringenin samples with sonication (black). (b) Effect of temperature on solubility of processed naringenin at different time points.

https://doi.org/10.1021/acsomega.2c04148
ACS Omega 2022, 7, 34476−34484

Table 1. Dissolution Study at pH-7.4 and 37 °C

s. no	sample	15 min	30 min	60 min	120 min	240 min	480 min	720 min
1	Ncrude	7.0%	7.49%	8.02%	8.52%	19.4%	33.6%	33.7%
2	N120	7.8%	9.6%	15.6%	20.1%	28.2%	43.1%	51.8%
3	N480	7.12%	8.1%	10.7%	16.2%	21%	30.6%	41%
4	N600	4.84%	9.7%	13.2%	18.3%	29.2%	35.3%	39.8%
5	N720	3.63%	6.06%	15.6%	32.4%	52%	75.1%	77.5%

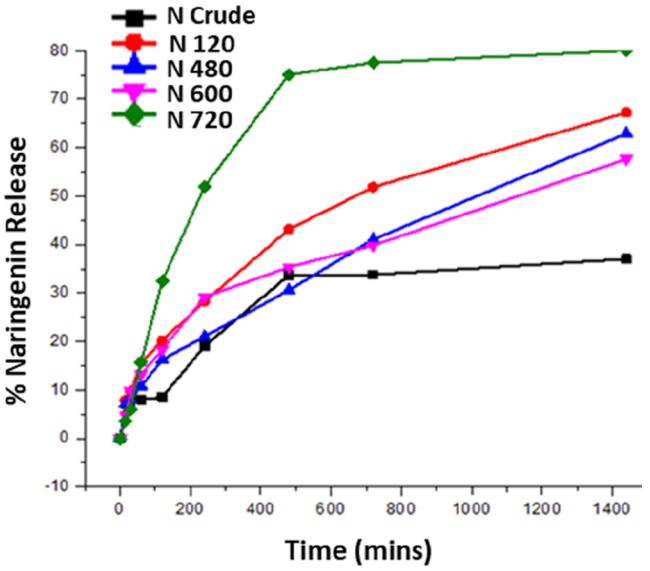

Figure 4. Dissolution study of naringenin at different milling times. In this graph, Ncrude, N120, N480, N600, and N720 show unprocessed naringenin, after 120 min of milling, after 480 min of milling, after 600 min of milling, after 720 min of milling, respectively.

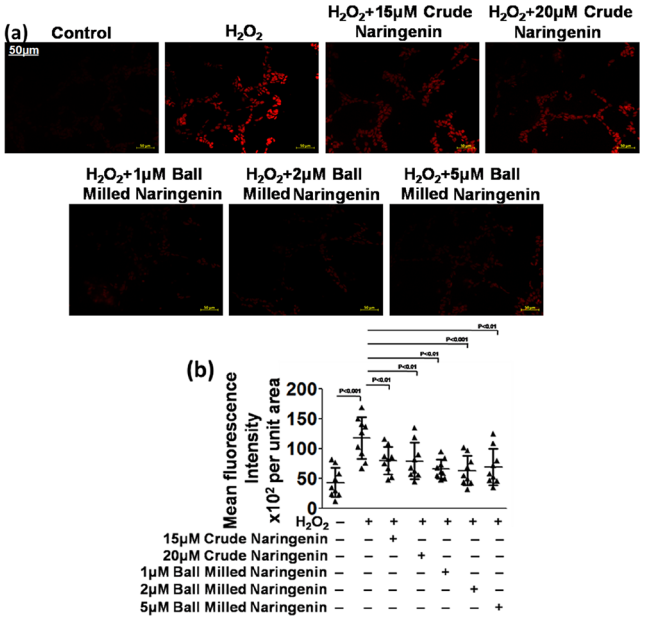

Figure 6. (a) DHE in the SH-SY5Y human neuroblastoma cell line and (b) its quantification.

case in the present study under consideration. The other significant reason is the slight change in the crystal structure of the bioactive compound, which also leads to the increased pharmacological efficacy of drugs.[32−35] It was observed that ball milling of the microcrystalline form could substantially convert this naive naringenin into its nanocrystalline form as seen under a scanning electron microscope. These results were in close corroboration of earlier reports, where the researchers employed SEM analyses to assess and establish the particle size of nanostructures obtained after the ball milling techniques.[36−39]

Once the particle size reduction of microcrystalline naringenin was confirmed by SEM analysis, the evaluation of any alteration in crystalline nature was assessed with XRD analysis of crude as well as milled forms. It was observed that there was no significant deviation of the naringenin form in its crystalline behavior as no major shift was noted down in the XRD peak patterns. These present outcomes are in complete compliance with earlier reports, where no considerable deviations in the crystalline behavior and crystal structures were observed after the ball milling process was undertaken on powders.[40−42] The characteristic peaks were present in the nanocrystalline form of naringenin, which confirmed its crystallinity. In the present report, these crystalline peaks were observed from the diffraction pattern of naringenin milled for 480 min and 720 min, which established that naringenin was in a crystalline form in both of these milled and crude samples (Figure 2).

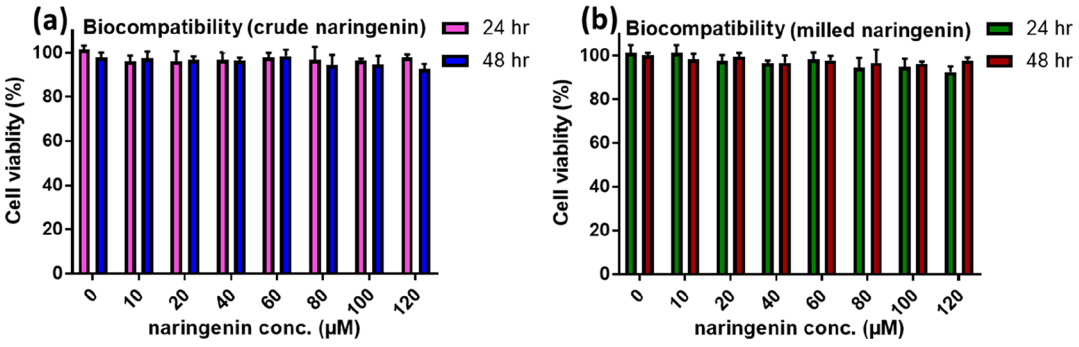

Figure 5. Biocompatibility study of the (a) crude or naive form and (b) nanosized form of naringenin as carried out in hTERT-BJ (human skin fibroblast) cell lines for a period of 24 and 48 h.

https://doi.org/10.1021/acsomega.2c04148
ACS Omega 2022, 7, 34476−34484

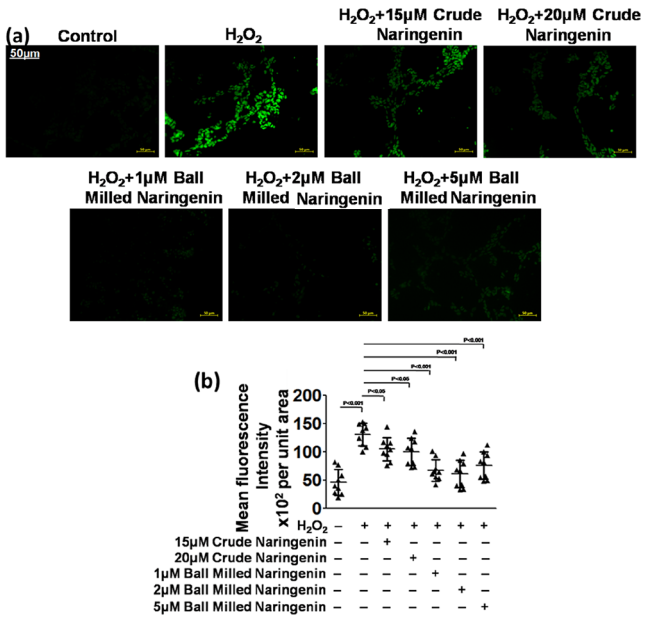

Figure 7. (a) DCFDA in the SH-SY5Y human neuroblastoma cell line and (b) its quantification.

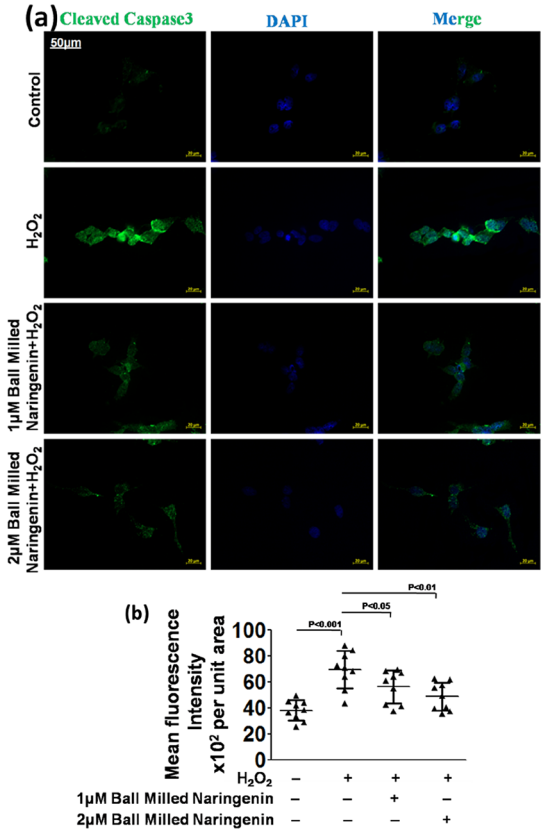

Figure 8. (a) Cleaved caspase-3 in the SH-SY5Y human neuroblastoma cell line and (b) its quantification.

The UV−visible spectrum of the crude or naïve (unmilled) form of naringenin and that of the ball-milled samples for 120, 240, 480, 600, and 720 min of processing were scanned, and solubility values were calculated from the λ_{max} values of absorbance. The resulting graph showed that the solubility of the naringenin enhanced as the milling time increased. Additionally, sonication of crude and milled naringenin samples further enhanced the solubility (Figure 3a). The values of solubility for unprocessed crude or naïve (unmilled) forms of naringenin and those of the sample ball-milled for 120, 240, 480, 600, and 720 min are 15.2, 36.9, 41.9, 43, 47, and 50% respectively. In this regard, various reports in the recent past have emphasized the quite pivotal role of ball milling in encountering the solubility-associated problems of the crude or naïve powdered forms and hence promoting its saturation solubilities.[24,43,44] Saturation solubilities of various samples of nanocrystalline naringenin that have been milled for corresponding time periods have been summarized in Table 1. For analyses of the effects of temperature variations on the saturation solubilities of all the ball-milled samples, nanocrystalline naringenin was made to get solubilized with stirring for 10 min. In the present study, the temperature was set at 27, 50, 75, and 100 °C. The value of solubility for crude naringenin and that of milled naringenin for 120, 240, 480, 600, and 720 min under different temperature conditions were evaluated and were found to be temperature-dependent as seen in Figure 3b. Solubility of the crude and milled naringenin samples also increased with an increase in temperature up to 100 °C. The solubility enhancement of milled naringenin samples is more (about 17.4% enhancement) as compared to that of crude naringenin (about 6% enhancement) in response to increased temperature (Figure 3b). Overall, the solubility of milled naringenin also depends upon milling, sonication, and temperature.

The drug release study was also carried out for the nanocrystalline naringenin via the dialysis bag method[45,46] for analyzing the release behavior in the physiological medium (Figure 4). The percentage release of unprocessed (crude) naringenin after 120, 480, 600, and 720 min of ball milling was found to be 33.7, 51.8, 41.0, 39.8, and 77.5%, respectively.

Once the drug release behavior of naringenin in the physiological medium was confirmed, its biocompatibility among the hTERT-BJ (human skin fibroblast) cell lines was carried out to establish its cytocompatibility among the normal cell lines. It was observed that both the crude naringenin and the milled naringenin were quite cytocompatible up to the doses of 120 μM each for the duration of 24 and 48 h, respectively (Figure 5a,b). We have chosen milled naringenin samples, which were processed up to the 720 min time point (N720). In all the subsequent experiments, we used the milled naringenin sample processed up to 720 min (N720) as at this time point, a marked increase in solubility of naringenin was observed. No appreciable or significant decline in the cell viability was observed up to 120 μM, which established that this in vitro safe dose of naringenin in its nanosized form could be applied for cellular studies. hTERT-BJ cells are fibroblast cells established from skin taken from the normal foreskin of a neonatal male. One of the chief applications includes toxicology research, which means that these cells are the most suitable for assessment and evaluations of the high-throughput screening of safety and toxicity of compounds and nanoformulations. These cells are of fibroblast origin, which is quite distinct from the epithelial origin, so in order to have an idea of what can be the probable safety or toxicological effects on different cells of the body, in case naringenin is used for in vivo studies, hTERT-BJ (human skin fibroblast) cells were employed for assessing the biocompatibility of the milled naringenin.

Dose-dependent pharmacological efficacy was determined in the human neuroblastoma cell lines in terms of the intracellular

https://doi.org/10.1021/acsomega.2c04148
ACS Omega 2022, 7, 34476−34484

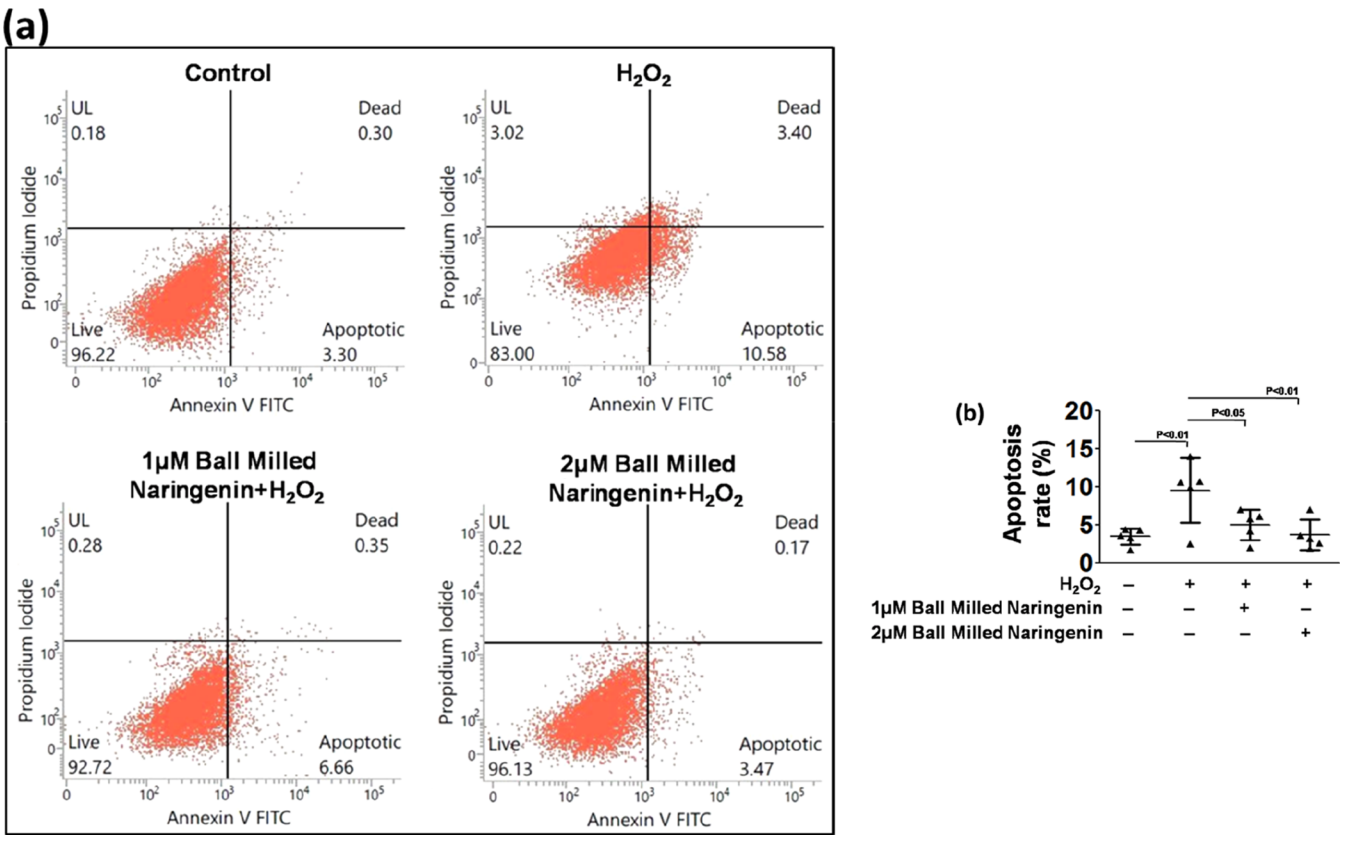

Figure 9. (a) Annexin-V PI flow cytometry for cell death of the SH-SY5Y human neuroblastoma cell line and (b) its quantification.

levels of ROS (including that of $O_2^{\bullet-}$) detection with an oxidation-sensitive fluorescent probing dihydroethidium (DHE) dye.[47,48] DHE assay can measure the levels of ROS directly in live cells. This assay employs DHE as a fluorescent probe for the detection of ROS generation and is specific for superoxide and hydrogen peroxide. ROS generation can be presented as total DHE fluorescence. Likewise, the DCFDA assay relies upon the diffusion of DCFDA into the cells. It is then deacetylated by cellular esterases to a non-fluorescent compound, which is later oxidized by ROS into 2′,7′-dichlorofluorescein (DCF). DCF is highly fluorescent and is detected by fluorescence spectroscopy with excitation/emission at 485 nm/535 nm. Since naringenin is a very potent anti-oxidant, its capability of neutralization of ROS in its rude or naïve or unmilled form as compared to that in the nanocrystalline form as well compared with the help of these assays. It was observed that the nanocrystalline form of naringenin was able to suppress the production of ROS in the SH-SY5Y human neuroblastoma cell line in a dose-dependent manner (Figure 6a). These outcomes showed close corroboration with other earlier reports, where nanoformulations were able to appreciably suppress the production or enhanced intracellular levels of ROS.[49,50] The corresponding quantification also demonstrated the significant lowering of ROS in the nanosized naringenin-treated human neuroblastoma cells (Figure 6b)

Another approach, viz., the DCFDA method was applied for the fluorescence-based detection of and measurements of hydroxyl, peroxyl, and other ROS activities within the human neuroblastoma cell line following the previous reported methods.[51,52] It was noted that the nanoparticulate form of naringenin was able to appreciably bring down the intracellular levels of ROS in a dose-dependent manner. The anti-oxidants and their nanoformulations have the capabilities and can appreciably decrease the intracellular ROS levels through their ROS scavenging effects (Figure 7a).[53,54] The corresponding quantification also demonstrated the significant lowering of ROS in the nanosized naringenin-treated human neuroblastoma cells (Figure 7b)

The pharmacological efficacy of nanocrystalline naringenin was also assessed in terms of the suppression of the apoptotic inducing enzyme, cleaved caspase-3. It was observed that the expression of cleaved caspase-3 was appreciably higher in the human neuroblastoma cells with higher levels of ROS. After the treatment of these cells with nanocrystalline naringenin, the cleaved caspase-3 expression level got considerably reduced in the human neuroblastoma cells (Figure 8a). This fluorescent expression level of cleaved caspase-3 was quantified, and a dose-dependent reduction in its expression was noted down in nanosized naringenin-treated human neuroblastoma cells (Figure 8b). In DCFDA assay, since the highest dose of 5 μM of nanosized naringenin was not able to show sufficiently significant results, it was omitted in the further experimentation and in the subsequent experiments, and only two doses of nanosized naringenin were employed, viz., 1 and 2 μM nanosized naringenin.

Flow cytometry analysis was used for assessing the apoptotic cell death due to the generation of ROS and anti-apoptotic effects of the nanoparticulate form of naringenin. It was observed that a higher dose of nanosized naringenin appreciably inhibited apoptotic cell death as compared to the lower dose as well as in comparison to the ROS-induced cell apoptosis group (Figure 9a). The comparative quantitative graphical representation also exhibited a significantly higher

https://doi.org/10.1021/acsomega.2c04148
ACS Omega 2022, 7, 34476−34484

apoptosis inhibition in human neuroblastoma cells in the 2 μM nanosized naringenin-treated group compared to that in the 1 μM nanosized naringenin-treated and untreated group (Figure 9b). In the DCFDA assay, since the highest dose of 5 μM nanosized naringenin was not able to exert sufficiently significant results, it was omitted in further experimentation and in the subsequent experiments, and only two doses of nanosized naringenin were employed, viz., 1 and 2 μM nanosized naringenin.

4. CONCLUSIONS

Despite being a promising natural antioxidant compound, naringenin has very low aqueous solubility. In this study, we used the high-energy ball milling method to reduce the size of naringenin without using any chemical. Size reduction leads to the increased solubility of naringenin, which depends upon milling time, sonication, and temperature. Interestingly, increased solubility resulted in an escalated antioxidant potential as demonstrated by its ability to reduce the level of ROS. Moreover, milled naringenin also demonstrated protective effects against H_2O_2-induced cell death. Milled naringenin exhibited 10 times better potency as compared to that of crude naringenin, which is mainly attributed to the reduction in the size of naringenin.

■ ASSOCIATED CONTENT

Supporting Information

The Supporting Information is available free of charge at https://pubs.acs.org/doi/10.1021/acsomega.2c04148.

Details of the materials and methods and other details of synthesis and characterization of naringenin and its biological evaluation (PDF)

■ AUTHOR INFORMATION

Corresponding Authors

Syed Shadab Raza − *Laboratory for Stem Cell & Restorative Neurology, Department of Biotechnology, Era's Lucknow Medical College Hospital, Lucknow, Uttar Pradesh 226003, India*; Email: drsyedshadabraza@gmail.com

Rehan Khan − *Chemical Biology Unit, Institute of Nano Science and Technology, Mohali, Punjab 140306, India*; orcid.org/0000-0002-2406-1129; Phone: +91-172-2210075; Email: rehankhan@inst.ac.in

Authors

Anas Ahmad − *Chemical Biology Unit, Institute of Nano Science and Technology, Mohali, Punjab 140306, India*; orcid.org/0000-0002-1105-7526

Ravi Prakash − *Laboratory for Stem Cell & Restorative Neurology, Department of Biotechnology, Era's Lucknow Medical College Hospital, Lucknow, Uttar Pradesh 226003, India*

Mohd Shahnawaz Khan − *Department of Biochemistry, College of Sciences, King Saud University, Riyadh 11451, Saudi Arabia*; orcid.org/0000-0002-4599-5924

Nojood Altwaijry − *Department of Biochemistry, College of Sciences, King Saud University, Riyadh 11451, Saudi Arabia*

Muhammad Nadeem Asghar − *Department of Medical Biology, University of Québec at Trois-Rivieres, Trois-Rivieres, Québec G9A 5H7, Canada*

Complete contact information is available at: https://pubs.acs.org/10.1021/acsomega.2c04148

Notes

The authors declare no competing financial interest.

■ ACKNOWLEDGMENTS

M.S.K. acknowledges the generous support from the Research Supporting Project (RSP-2021/352) by King Saud University, Riyadh, Kingdom of Saudi Arabia.

■ REFERENCES

(1) Malysheva, A.; Ivask, A.; Doolette, C. L.; Voelcker, N. H.; Lombi, E. Cellular Binding, Uptake and Biotransformation of Silver Nanoparticles in Human T Lymphocytes. *Nat. Nanotechnol.* **2021**, *16*, 926−932.

(2) Lu, G. J.; Farhadi, A.; Szablowski, J. O.; Lee-Gosselin, A.; Barnes, S. R.; Lakshmanan, A.; Bourdeau, R. W.; Shapiro, M. G. Acoustically Modulated Magnetic Resonance Imaging of Gas-Filled Protein Nanostructures. *Nat. Mater.* **2018**, *17*, 456−463.

(3) Nogrady, B. How Nanotechnology Can Flick the Immunity Switch. *Nature* **2021**, *595*, S18−S19.

(4) Phillips, I. D. J. Induction of a Light Requirement for the Germination of Lettuce Seed by Naringenin, and Its Removal by Gibberellic Acid. *Nature* **1961**, *192*, 240−241.

(5) Ahmad, A.; Fauzia, E.; Kumar, M.; Mishra, R. K.; Kumar, A.; Khan, M. A.; Raza, S. S.; Khan, R. Gelatin-Coated Polycaprolactone Nanoparticle-Mediated Naringenin Delivery Rescue Human Mesenchymal Stem Cells from Oxygen Glucose Deprivation-Induced Inflammatory Stress. *ACS Biomater. Sci. Eng.* **2019**, *5*, 683−695.

(6) Jeon, S.-M.; Kim, H. K.; Kim, H.-J.; Do, G.-M.; Jeong, T.-S.; Park, Y. B.; Choi, M.-S. Hypocholesterolemic and Antioxidative Effects of Naringenin and Its Two Metabolites in High-Cholesterol Fed Rats. *Transl. Res.* **2007**, *149*, 15−21.

(7) Ahmad, A.; Bulani, Y.; Sharma, S. S. Naringenin Shows Ameliorative Effects in Isoproterenol-Induced Myocardial Infarction. *12th Annual Conference of International Society of Heart Research (ISHRCON)*; Jawaharlal Nehru University, 2015.

(8) Jung, U. J.; Kim, H. J.; Lee, J. S.; Lee, M. K.; Kim, H. O.; Park, E. J.; Kim, H. K.; Jeong, T. S.; Choi, M. S. Naringin Supplementation Lowers Plasma Lipids and Enhances Erythrocyte Antioxidant Enzyme Activities in Hypercholesterolemic Subjects. *Clin. Nutr.* **2003**, *22*, 561−568.

(9) Coelho, R. C. L. A.; Hermsdorff, H. H. M.; Bressan, J. Anti-Inflammatory Properties of Orange Juice: Possible Favorable Molecular and Metabolic Effects. *Plant Foods Hum. Nutr.* **2013**, *68*, 1−10.

(10) Chen, C.; Jie, X.; Ou, Y.; Cao, Y.; Xu, L.; Wang, Y.; Qi, R. Nanoliposome Improves Inhibitory Effects of Naringenin on Nonalcoholic Fatty Liver Disease in Mice. *Nanomedicine* **2017**, *12*, 1791−1800.

(11) Podder, B.; Song, H.-Y.; Kim, Y.-S. Naringenin Exerts Cytoprotective Effect Against Paraquat-Induced Toxicity in Human Bronchial Epithelial BEAS-2B Cells Through NRF2 Activation. *J. Microbiol. Biotechnol.* **2014**, *24*, 605−613.

(12) Li, Q.; Wang, Y.; Zhang, L.; Chen, L.; Du, Y.; Ye, T.; Shi, X. Naringenin Exerts Anti-Angiogenic Effects in Human Endothelial Cells: Involvement of ERRα/VEGF/KDR Signaling Pathway. *Fitoterapia* **2016**, *111*, 78−86.

(13) Sandhu, P. S.; Kumar, R.; Beg, S.; Jain, S.; Kushwah, V.; Katare, O. P.; Singh, B. Natural Lipids Enriched Self-Nano-Emulsifying Systems for Effective Co-Delivery of Tamoxifen and Naringenin: Systematic Approach for Improved Breast Cancer Therapeutics. *Nanomed.: Nanotechnol. Biol. Med.* **2017**, *13*, 1703−1713.

(14) Bhia, M.; Motallebi, M.; Abadi, B.; Zarepour, A.; Pereira-Silva, M.; Saremnejad, F.; Santos, A. C.; Zarrabi, A.; Melero, A.; Jafari, S. M.; Shakibaei, M. Naringenin Nano-Delivery Systems and Their Therapeutic Applications. *Pharmaceutics* **2021**, *13*, 291.

(15) El-Eskandarany, M. S.; Al-Hazza, A.; Al-Hajji, L. A.; Ali, N.; Al-Duweesh, A. A.; Banyan, M.; Al-Ajmi, F. Mechanical Milling: A

Superior Nanotechnological Tool for Fabrication of Nanocrystalline and Nanocomposite Materials. *Nanomaterials* **2021**, *11*, 2484.
(16) Van Swygenhoven, H.; Derlet, P. M.; Frøseth, A. G. Stacking Fault Energies and Slip in Nanocrystalline Metals. *Nat. Mater.* **2004**, *3*, 399−403.
(17) Salah, N.; Habib, S. S.; Khan, Z. H.; Memic, A.; Azam, A.; Al-Hamedi, E.; Zahed, N.; Habib, S. High-Energy Ball Milling Technique for ZnO Nanoparticles as Antibacterial Material. *Int. J. Nanomed.* **2011**, *6*, 863−869.
(18) Glushenkov, A. M.; Zhang, H. Z.; Chen, Y. Reactive Ball Milling to Produce Nanocrystalline ZnO. *Mater. Lett.* **2008**, *62*, 4047−4049.
(19) Dong, Z.; Wang, R.; Wang, M.; Meng, Z.; Wang, X.; Han, M.; Guo, Y.; Wang, X. Preparation of Naringenin Nanosuspension and Its Antitussive and Expectorant Effects. *Molecules* **2022**, *27*, 741.
(20) Kandeil, M. A.; Mohammed, E. T.; Radi, R. A.; Khalil, F.; Abdel-Razik, A.-R. H.; Abdel-Daim, M. M.; Safwat, G. M. Nano-naringenin and Vitamin E Ameliorate Some Behavioral, Biochemical, and Brain Tissue Alterations Induced by Nicotine in Rats. *J. Toxicol.* **2021**, *2021*, 1−15.
(21) Zhang, G.; Sun, G.; Guan, H.; Li, M.; Liu, Y.; Tian, B.; He, Z.; Fu, Q. Naringenin Nanocrystals for Improving Anti-Rheumatoid Arthritis Activity. *Asian J. Pharm. Sci.* **2021**, *16*, 816−825.
(22) Gera, S.; Talluri, S.; Rangaraj, N.; Sampathi, S. Formulation and Evaluation of Naringenin Nanosuspensions for Bioavailability Enhancement. *AAPS PharmSciTech* **2017**, *18*, 3151−3162.
(23) Han, G.-F.; Li, F.; Rykov, A. I.; Im, Y.-K.; Yu, S.-Y.; Jeon, J.-P.; Kim, S.-J.; Zhou, W.; Ge, R.; Ao, Z.; Shin, T. J.; Wang, J.; Jeong, H. Y.; Baek, J.-B. Abrading Bulk Metal into Single Atoms. *Nat. Nanotechnol.* **2022**, *17*, 403−407.
(24) Pawelke, R. Ball Milling as a Tool Towards Solubility Problems in Synthesis—Simple and Solvent-Free Preparation of K[B(CN)4]. *Nat. Preced.* **2011**, 1.
(25) Lampronti, G. I.; Michalchuk, A. A. L.; Mazzeo, P. P.; Belenguer, A. M.; Sanders, J. K. M.; Bacchi, A.; Emmerling, F. Changing the Game of Time Resolved X-Ray Diffraction on the Mechanochemistry Playground by Downsizing. *Nat. Commun.* **2021**, *12*, 6134.
(26) Boldyreva, E. Defogging the View through a Milling Jar. *Nat. Chem.* **2022**, *14*, 10−12.
(27) Calka, A.; Wexler, D. Mechanical Milling Assisted by Electrical Discharge. *Nature* **2002**, *419*, 147−151.
(28) Eze, A. A.; Sadiku, E. R.; Kupolati, W. K.; Snyman, J.; Ndambuki, J. M.; Jamiru, T.; Durowoju, M. O.; Ibrahim, I. D.; Shongwe, M. B.; Desai, D. A. Wet Ball Milling of Niobium by Using Ethanol, Determination of the Crystallite Size and Microstructures. *Sci. Rep.* **2021**, *11*, 22422.
(29) Narayan, R.; Pednekar, A.; Bhuyan, D.; Gowda, C.; K, K.; Nayak, U. Y. A Top-down Technique to Improve the Solubility and Bioavailability of Aceclofenac: In Vitro and in Vivo Studies. *Int. J. Nanomed.* **2017**, *12*, 4921−4935.
(30) Deng, J.; Sun, F.; Wang, Y.; Sui, Z.; She, W.; Zhai, C.; Wang, Y. Effect of Particle Size on Solubility, Dissolution Rate, and Oral Bioavailability: Evaluation Using Coenzyme Q10 as Naked Nanocrystals. *Int. J. Nanomed.* **2012**, *7*, 5733−5744.
(31) Patrick, A. D.; Young, E.; Ellis, C.; Rodeck, C. H. Multiple Sulphatase Deficiency: Prenatal Diagnosis Using Chorionic Villi. *Prenatal Diagn.* **1988**, *8*, 303−306.
(32) Yamamoto, O.; Komatsu, M.; Sawai, J.; Nakagawa, Z. Effect of Lattice Constant of Zinc Oxide on Antibacterial Characteristics. *J. Mater. Sci.: Mater. Med.* **2004**, *15*, 847−851.
(33) Premanathan, M.; Karthikeyan, K.; Jeyasubramanian, K.; Manivannan, G. Selective Toxicity of ZnO Nanoparticles toward Gram-Positive Bacteria and Cancer Cells by Apoptosis through Lipid Peroxidation. *Nanomed.: Nanotechnol. Biol. Med.* **2011**, *7*, 184−192.
(34) Ma, X.-Y.; Zhang, W.-D. Effects of Flower-like ZnO Nanowhiskers on the Mechanical, Thermal and Antibacterial Properties of Waterborne Polyurethane. *Polym. Degrad. Stab.* **2009**, *94*, 1103−1109.
(35) Yamamoto, O.; Sawai, J.; Sasamoto, T. Change in Antibacterial Characteristics with Doping Amount of ZnO in MgO−ZnO Solid Solution. *Int. J. Inorg. Mater.* **2000**, *2*, 451−454.
(36) Han, G.-F.; Li, F.; Chen, Z.-W.; Coppex, C.; Kim, S.-J.; Noh, H.-J.; Fu, Z.; Lu, Y.; Singh, C. V.; Siahrostami, S.; Jiang, Q.; Baek, J.-B. Mechanochemistry for Ammonia Synthesis under Mild Conditions. *Nat. Nanotechnol.* **2021**, *16*, 325−330.
(37) Humphry-Baker, S. A.; Garroni, S.; Delogu, F.; Schuh, C. A. Melt-Driven Mechanochemical Phase Transformations in Moderately Exothermic Powder Mixtures. *Nat. Mater.* **2016**, *15*, 1280−1286.
(38) Zhu, X.; Zhang, T.; Jiang, D.; Duan, H.; Sun, Z.; Zhang, M.; Jin, H.; Guan, R.; Liu, Y.; Chen, M.; Ji, H.; Du, P.; Yan, W.; Wei, S.; Lu, Y.; Yang, S. Stabilizing Black Phosphorus Nanosheets via Edge-Selective Bonding of Sacrificial C60 Molecules. *Nat. Commun.* **2018**, *9*, 41771−41779.
(39) Park, M.; Schuh, C. A. Accelerated Sintering in Phase-Separating Nanostructured Alloys. *Nat. Commun.* **2015**, *6*, 68581−68586.
(40) Friščić, T.; Halasz, I.; Beldon, P. J.; Belenguer, A. M.; Adams, F.; Kimber, S. A. J.; Honkimäki, V.; Dinnebier, R. E. Real-Time and in Situ Monitoring of Mechanochemical Milling Reactions. *Nat. Chem.* **2013**, *5*, 66−73.
(41) Katsenis, A. D.; Puškarić, A.; Štrukil, V.; Mottillo, C.; Julien, P. A.; Užarević, K.; Pham, M.-H.; Do, T.-O.; Kimber, S. A. J.; Lazić, P.; Magdysyuk, O.; Dinnebier, R. E.; Halasz, I.; Friščić, T. In Situ X-Ray Diffraction Monitoring of a Mechanochemical Reaction Reveals a Unique Topology Metal-Organic Framework. *Nat. Commun.* **2015**, *6*, 66621−66628.
(42) Li, T.; Heenan, T. M. M.; Rabuni, M. F.; Wang, B.; Farandos, N. M.; Kelsall, G. H.; Matras, D.; Tan, C.; Lu, X.; Jacques, S. D. M.; Brett, D. J. L.; Shearing, P. R.; Di Michiel, M.; Beale, A. M.; Vamvakeros, A.; Li, K. Design of Next-Generation Ceramic Fuel Cells and Real-Time Characterization with Synchrotron X-Ray Diffraction Computed Tomography. *Nat. Commun.* **2019**, *10*, 14971−15011.
(43) Zhang, P.; Wang, L.; Yang, S.; Schott, J. A.; Liu, X.; Mahurin, S. M.; Huang, C.; Zhang, Y.; Fulvio, P. F.; Chisholm, M. F.; Dai, S. Solid-State Synthesis of Ordered Mesoporous Carbon Catalysts via a Mechanochemical Assembly through Coordination Cross-Linking. *Nat. Commun.* **2017**, *8*, 15020.
(44) León, V.; Rodriguez, A. M.; Prieto, P.; Prato, M.; Vázquez, E. Exfoliation of Graphite with Triazine Derivatives under Ball-Milling Conditions: Preparation of Few-Layer Graphene via Selective Noncovalent Interactions. *ACS Nano* **2014**, *8*, 563−571.
(45) Ahmad, A.; Ansari, Md. M.; Mishra, R. K.; Kumar, A.; Vyawahare, A.; Verma, R. K.; Raza, S. S.; Khan, R. Enteric-Coated Gelatin Nanoparticles Mediated Oral Delivery of 5-Aminosalicylic Acid Alleviates Severity of DSS-Induced Ulcerative Colitis. *Mater. Sci. Eng., C* **2021**, *119*, 111582.
(46) Ahmad, A.; Ansari, M. M.; Kumar, A.; Bishnoi, M.; Raza, S. S.; Khan, R. Aminocellulose—Grafted Polycaprolactone-Coated Core−Shell Nanoparticles Alleviate the Severity of Ulcerative Colitis: A Novel Adjuvant Therapeutic Approach. *Biomater. Sci.* **2021**, *9*, 5868−5883.
(47) Dikalov, S. I.; Harrison, D. G. Methods for Detection of Mitochondrial and Cellular Reactive Oxygen Species. *Antioxid. Redox Signaling* **2014**, *20*, 372−382.
(48) Griendling, K. K.; Touyz, R. M.; Zweier, J. L.; Dikalov, S.; Chilian, W.; Chen, Y.-R.; Harrison, D. G.; Bhatnagar, A. Measurement of Reactive Oxygen Species, Reactive Nitrogen Species, and Redox-Dependent Signaling in the Cardiovascular System. *Circ. Res.* **2016**, *119*, e39−e75.
(49) Wang, Y.; Li, L.; Zhao, W.; Dou, Y.; An, H.; Tao, H.; Xu, X.; Jia, Y.; Lu, S.; Zhang, J.; Hu, H. Targeted Therapy of Atherosclerosis by a Broad-Spectrum Reactive Oxygen Species Scavenging Nanoparticle with Intrinsic Anti-Inflammatory Activity. *ACS Nano* **2018**, *12*, 8943−8960.
(50) Yim, D.; Lee, D.-E.; So, Y.; Choi, C.; Son, W.; Jang, K.; Yang, C.-S.; Kim, J.-H. Sustainable Nanosheet Antioxidants for Sepsis

https://doi.org/10.1021/acsomega.2c04148
ACS Omega 2022, 7, 34476−34484

Therapy via Scavenging Intracellular Reactive Oxygen and Nitrogen Species. *ACS Nano* **2020**, *14*, 10324−10336.
(51) Eruslanov, E.; Kusmartsev, S. Identification of ROS Using Oxidized DCFDA and Flow-Cytometry. *Methods Mol. Biol.* **2010**, *594*, 57−72.
(52) Figueroa, D.; Asaduzzaman, M.; Young, F. Real Time Monitoring and Quantification of Reactive Oxygen Species in Breast Cancer Cell Line MCF-7 by 2′,7′-Dichlorofluorescin Diacetate (DCFDA) Assay. *J. Pharmacol. Toxicol. Methods* **2018**, *94*, 26−33.
(53) Capasso, M.; Bhamrah, M. K.; Henley, T.; Boyd, R. S.; Langlais, C.; Cain, K.; Dinsdale, D.; Pulford, K.; Khan, M.; Musset, B.; Cherny, V. V.; Morgan, D.; Gascoyne, R. D.; Vigorito, E.; DeCoursey, T. E.; MacLennan, I. C. M.; Dyer, M. J. S. HVCN1 Modulates BCR Signal Strength via Regulation of BCR-Dependent Generation of Reactive Oxygen Species. *Nat. Immunol.* **2010**, *11*, 265−272.
(54) Punjabi, A.; Wu, X.; Tokatli-Apollon, A.; El-Rifai, M.; Lee, H.; Zhang, Y.; Wang, C.; Liu, Z.; Chan, E. M.; Duan, C.; Han, G. Amplifying the Red-Emission of Upconverting Nanoparticles for Biocompatible Clinically Used Prodrug-Induced Photodynamic Therapy. *ACS Nano* **2014**, *8*, 10621−10630.

https://doi.org/10.1021/acsomega.2c04148
ACS Omega 2022, 7, 34476−34484